

Pure quadrupole resonances have also been observed when a perturbing magnetic field applied perpendicular to the axis of the electric field in the absence of a field  $H_0$  has induced transitions leading to absorption of radio-frequency power.

#### 8.5.9 The measurements of quadrupole moments by paramagnetic resonances

The technique of Purcell described in section 8.5.6 has been applied to paramagnetic atoms. The much larger magnetic moment of the atom places the Larmor frequencies, and hence the resonant frequencies, in the microwave range. The effect of the nuclear spin is then to produce hyperfine splitting in the atomic resonances. By observing the degree of splitting as a function of  $H_0$ , diagrams of the type encountered in optical hyperfine splitting (see Figure 43, p. 137) are constructed. By comparing these with the theory of hyperfine splitting outlined above, the effect of the quadrupole moment can be detected and values of  $B$  estimated.

#### 8.6 Summary

Spins of nuclei can be measured by several techniques and can be regarded as very well established for ground states of stable nuclei. In some cases the techniques can be applied to give a direct measurement of spin for unstable nuclei of suitably long half-life.

Magnetic moments can be measured with high precision, a precision limited in practice by the accuracy with which the internal and induced field produced by the orbital electrons at the nucleus can be calculated.

With respect to quadrupole moments the situation is very much less satisfactory. In certain cases  $B$  can be measured directly; in other cases it can be measured as a deviation of hyperfine structure from that expected on the basis of magnetic dipole moments alone. However, the deduction of  $Q$  from  $B$  is very uncertain because of the lack of knowledge of the internal electric field gradients at the nucleus. The ratio of  $Q$  for two isotopes is known with better accuracy on the assumption that the internal electric field gradient is the same for both isotopes.

As we shall see later, information about both electric and magnetic moments of nuclei comes from the study of transitions between their excited states. It is to that source that at present one has to look for better information about the electric quadrupole moment.

Values of spins, magnetic dipole moments and quadrupole moments for stable nuclei are listed in Appendix A.

## Chapter 9 The Collective Model

### 9.1 Introduction

We recall that the discussion of section 6.10 showed that a good account of the ground-state spin of nuclei can be given in terms of the shell model. In that account it is assumed that nucleons of the same kind form pairs, their angular momenta coupling so that the resultant angular momentum of the pair is zero. In the case of (even, even) nuclei there is complete pairing and hence the spin predicted by the model is zero. This, without known exception, is in agreement with measured spins. In the case of odd- $A$  nuclei there is always a nucleon of one type left unpaired. The nuclear spin then is assumed to arise entirely from the motion of this unpaired nucleon. In the case of (odd, odd) nuclei there is an unpaired nucleon of each kind and the nuclear spin has a contribution from the motion of each of these. The satisfactory agreement of this account of nuclear spins with experimental observations argues strongly for the validity of the shell model.

The attempt to extend the ideas of the shell model to explain magnetic dipole moments met, as we saw in section 7.3, with only limited success. It is true that (even, even) nuclei have zero magnetic moment, as well as zero spin, as would be expected on the assumption that the nucleons form pairs. However, in the case of odd- $A$  nuclei, we see from Figures 31 and 32 (pp. 110-12) that, with few exceptions, the measured magnetic dipole moments are significantly smaller than the 'single-particle' predictions. One must conclude that in these cases the paired nucleons in the 'core' are not exactly compensating each others' magnetic moments but are making a contribution to the total dipole moment, this despite the fact that they do compensate each others' angular momentum. It is however to be noted that the main contribution to the magnetic moment still arises from the single particle.

The situation *vis-à-vis* the predictions of the shell model and the experimental facts is less satisfactory when we turn to electric quadrupole moments. The quadrupole moment is taken as a measure of the departure of the charge distribution from spherical symmetry. If a nucleus has a closed shell of protons it has no total angular momentum and hence no distinctive axis. It is therefore expected to exhibit spherical symmetry of charge. If we now take the case of one proton outside a closed shell then, unless that proton be in an  $s$ -state, its equivalent charge distribution will not be spherically symmetric and a nuclear electric quadrupole moment would be expected to result. Consider now a second

proton outside the shell. If this pairs with the first to give zero total angular momentum, then again, on the above argument, spherical symmetry is restored. If a third proton be added then, providing it does not split the existing pair, its situation will be as for the first proton, that is, it should give rise to a quadrupole moment calculable from its wave function. This argument can be extended to show that spherical symmetry is to be expected when the number of protons is even and

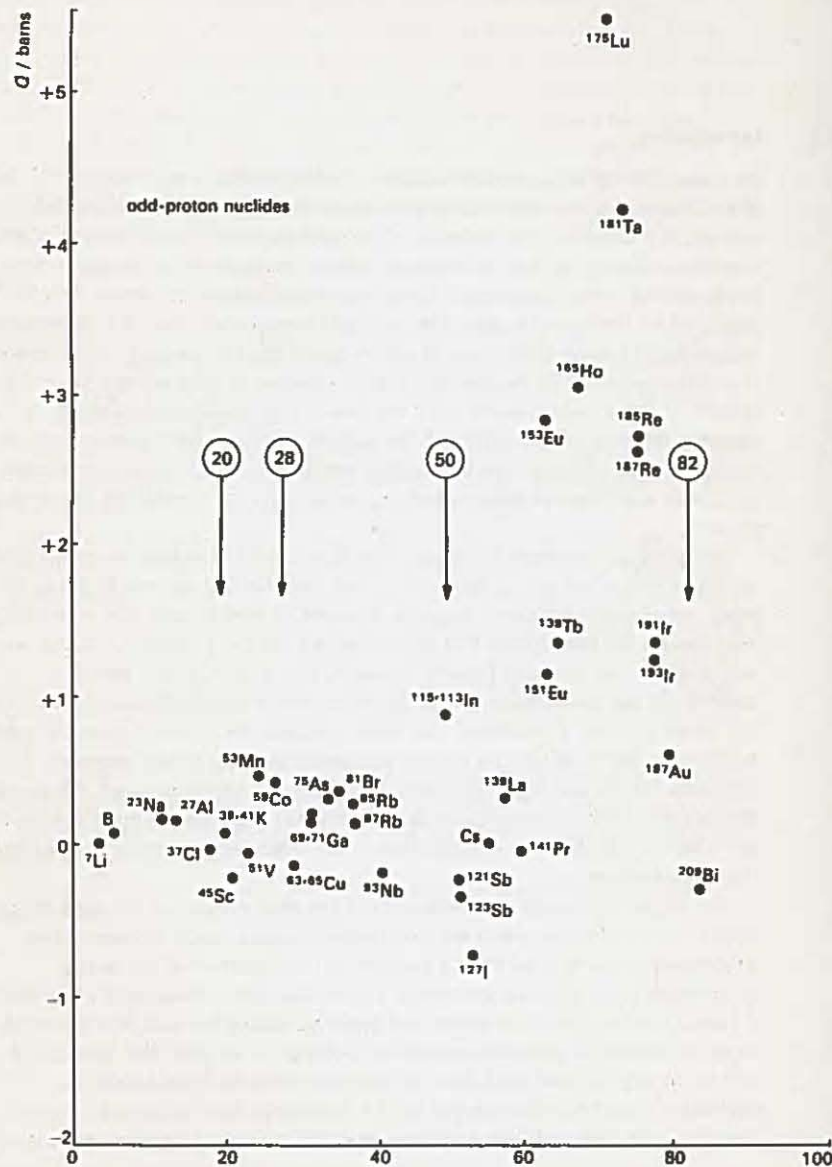


Figure 51(a) Plot of measured quadrupole moments of odd-A, odd-Z nuclei Z

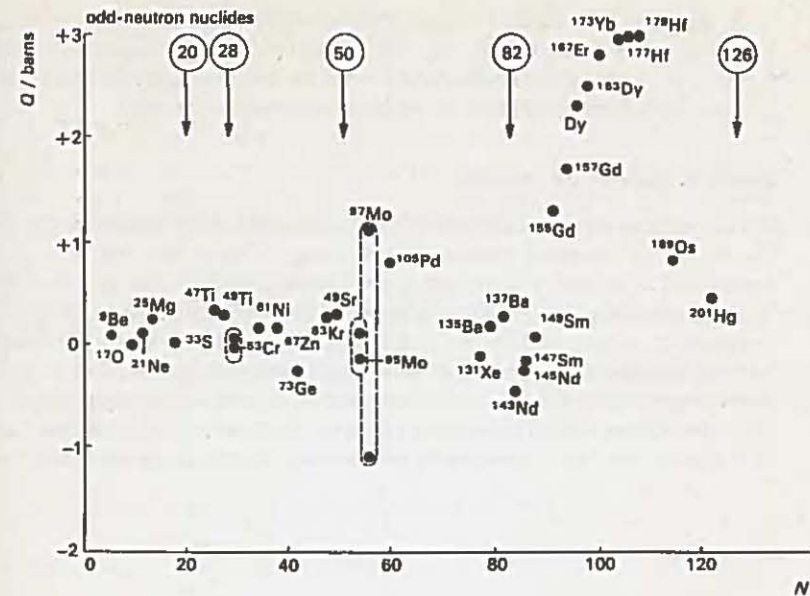


Figure 51(b) Plot of measured quadrupole moments of odd-A, odd-N nuclei  
 a departure from symmetry of charge distribution, associated with one proton, is to be expected when the proton number is odd. Now in a nucleus of radius, say, eight fermis, a single proton can at the most give rise to a quadrupole moment of 0.128 barns (this follows from the application of equation 7.12 to this simple situation where  $r = z$ ). On the other hand, quadrupole moments as large as eight barns have been measured. Although these measurements, as was pointed out in section 8.6, are subject to considerable experimental uncertainties, nevertheless it is clear that there is an order-of-magnitude discrepancy at least between the single-particle-model prediction and the measurements. It is also to be noted from Figure 51 that the discrepancy is greatest when the proton number is midway between closed shells. As a further departure from shell-model expectations, odd-A nuclei having paired protons but an unpaired neutron exhibit quadrupole moments.

Nuclei which have shells half-filled not only show serious departure from shell-model predictions in respect of quadrupole moments, but have as a characteristic an excited state, not much above the ground state in energy, de-exciting by electric quadrupole transition to the ground state. The transition rate is higher than would be expected from single-particle considerations and is an indication that a large electric quadrupole moment is involved in the process. These considerations led Bohr and Mottelson (1953) to develop the collective model of the nucleus, which we now proceed to outline. This model attempts to extend the shell model rather than to replace it. It adds to the shell model some features of the liquid-drop model and, as it borrowed from both of these extreme nuclear models, it was originally sometimes referred to as the *unified model*.

In setting up the collective model a close analogy was maintained with the behaviour of the diatomic molecule as described by quantum mechanics. To make it clear how the ideas and nomenclature arose, we begin by outlining briefly the relevant features and properties of the diatomic molecular system.

## 9.2 Theory of the diatomic molecule

In Figure 52 we represent a simple diatomic molecule having nuclei at A and B. The theoretical treatment assumes that the energy of the system may be represented as the sum of three terms. The first of these is the energy of rotation of the system about the axis PQ; the second is the energy of vibration of the nuclei which, if their separation  $d$  is disturbed, are assumed to vibrate with simple harmonic motion about their equilibrium separation; the third and final term is due to the energy of the orbital electrons associated with one or other of the nuclei or orbiting both. The moment of inertia about the axis AB is assumed to be negligibly small and consequently no allowance is made for rotation about AB.

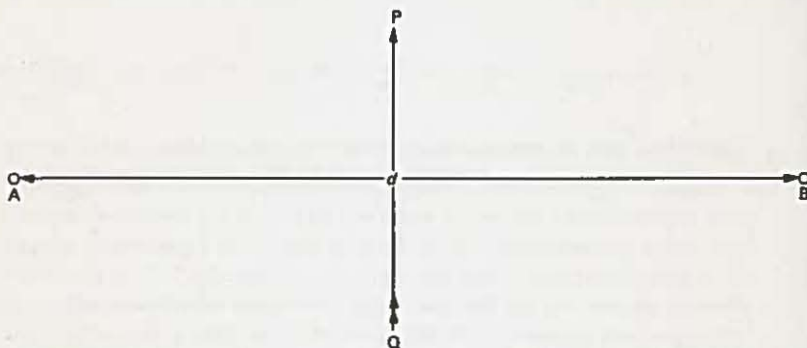


Figure 52 Schematic diagram of a diatomic molecule with atoms situated at A and B

We first consider the rotational energy about PQ. If the moment of inertia about the axis is  $\mathcal{I}$  then we can write

$$E_{\text{rot}} = \frac{1}{2} \mathcal{I} \omega^2,$$

where  $\omega$  is the angular velocity of the system about the axis PQ. The angular momentum about that axis will be  $\mathcal{I}\omega$  and we note that, from classical mechanics, we can write

$$E_{\text{rot}} = \frac{(\mathcal{I}\omega)^2}{2\mathcal{I}}.$$

When the system is treated as a quantum-mechanical rotator, we assign to it, when it is in a stationary state, a quantum number  $R$  which is related to the quantized angular momentum of rotation by the equation

$$\text{Angular momentum about axis of rotation} = \sqrt{R(R+1)} \hbar.$$

In the quantum-mechanical treatment we then have

$$E_{\text{rot}} = \frac{R(R+1)\hbar^2}{2\mathcal{I}}. \quad 9.1$$

If now the molecule has an electric-dipole moment it will be capable of interacting with the electromagnetic field. It may therefore radiate energy or it may absorb energy from the field thereby making a transition between states differing by  $\pm 1$  in  $R$ -value. The energy of quantum radiated or absorbed will be given by

$$(h\nu)_{\text{rot}} = E_{\text{rot}} = \frac{[R(R+1) - (R-1)R]\hbar^2}{2\mathcal{I}} = \frac{R\hbar^2}{\mathcal{I}}. \quad 9.2$$

Let us take the HCl molecule as an example to which this theory should apply. The separation  $d$  will be of the order of  $10^{-10}$  m. Hence, taking the moment of inertia about an axis through G, the centre of mass, perpendicular to the line joining the nuclei we have

$$\mathcal{I} = (M_C x_C^2 + M_H x_H^2) = \frac{35}{36} M_H d^2 \approx 1.6 \times 10^{-44} \text{ g m}^2.$$

$$\text{Hence } \nu_{\text{rot}} = \frac{R\hbar}{2\pi\mathcal{I}} \approx R \times 10^{-12} \text{ Hz.}$$

This frequency, for small values of  $R$ , corresponds to the far infrared region of the electromagnetic spectrum. When this spectral region is examined in the absorption spectrum of HCl, a sequence of lines, listed by wave number (i.e.  $k = 1/\lambda = \nu/c$ ) in Table 5, is found. The difference in wave numbers, apart

Table 5: Absorption Spectrum of HCl in the Far Infrared.

$k$ (observed) $\times$ mm	$\Delta k$ $\times$ mm	$\frac{k}{\Delta k}$	$k$ (calculated) $\times$ mm	$[k$ (calculated) $- k$ (observed)] $\times$ mm
8.303	$2 \times 2.063$	4.06	(8.303)	—
...				
12.430	2.073	6.07	12.455	0.025
14.503	2.048	7.08	14.530	0.027
16.551	2.035	8.08	16.606	0.055
18.586	2.052	9.08	18.682	0.096
20.638	2.012	10.08	20.758	0.120
22.650		(11.06)	22.833	0.183

from that between the first and second entries, is seen to be effectively constant. The exception is so close to twice this constant difference as to suggest that there is a line missing. If the interpretation in terms of rotation is correct, then

$$k_{\text{rot}} = \frac{\nu_{\text{rot}}}{c} = \frac{R_{\text{rot}} \hbar}{2\pi\mathcal{I}c}$$

and hence  $\Delta k_{\text{rot}} = \frac{\hbar}{2\pi \mathcal{I} c}$ .

It follows that

$$\frac{k_{\text{rot}}}{\Delta k_{\text{rot}}} = R_{\text{rot}},$$

where  $R_{\text{rot}}$  should be integral.

From column three of the table it can be seen how well this prediction is borne out. If we now take the nearest integers and use the first wave number we can calculate the wave numbers of the other lines. It can be seen that the agreement is good but that there is a discrepancy growing systematically as shown in the final column of the table. This discrepancy is understandable in terms of the simple rotator model. As we proceed to higher rotational states, the centrifugal force will increase and this will tend to stretch the molecule. The increased separation will lead to an increase in  $\mathcal{I}$  and, according to equation 9.1, a decrease in the expected value of  $E_{\text{rot}}$ .

We can use the spectral information to find accurate, rather than order-of-magnitude, values of  $I$  and  $d$ . We have

$$\mathcal{I} = \frac{R\hbar}{2\pi \nu_{\text{rot}}} = \frac{R\hbar}{2\pi c k_{\text{rot}}} = 2.7 \times 10^{-44} \text{ g m}^2.$$

It follows that  $d = \sqrt{\frac{36\mathcal{I}}{35M_H}} = 1.29 \times 10^{-10} \text{ m}.$

There is thus seen to be impressive agreement between the spectroscopic data and the predictions of the rotator model.

The existence of rotational states should affect the thermodynamic properties of a gas consisting of diatomic molecules. From the equipartitioning of energy in kinetic theory, it follows that  $C_v$ , the specific heat of a gas, is  $\frac{1}{2}nR$ , where  $R$  is the gas constant and  $n$  the number of degrees of freedom possessed by the molecules. If the rotational states enter into the equipartitioning of the energy they will add two additional degrees of freedom, since rotation can take place independently about two axes perpendicular to AB in Figure 52. The extent to which the rotational states take up thermal energy will be dictated by the Boltzman factor. This ensures that the rotational states are negligibly populated when

$$kT \ll (h\nu)_{\text{rot}} \approx \frac{\hbar^2}{\mathcal{I}}.$$

When however  $kT \approx \frac{\hbar^2}{\mathcal{I}}$  (i.e.  $T \approx \frac{\hbar^2}{\mathcal{I}k} = 30 \text{ K}$ ),

then  $n$  should increase from 3 to 5. In fact  $C_v$  is observed to increase from  $\frac{3}{2}R$  to  $\frac{5}{2}R$  in this temperature range, further supporting the validity of the rotator model.

We now turn to the vibrational energy. If the 'restoring' force is proportional to the change in the separation distance of the nuclei, then the system should

correspond to a quantum-mechanical oscillator. Such an oscillator has a set of stationary states of energy given by

$$E_{\text{vib}} = (n + \frac{1}{2})(h\nu)_{\text{vib}}, \tag{9.3}$$

where  $n$  is an integer. A knowledge of the restoring-force constant would enable  $(h\nu)_{\text{vib}}$  to be calculated. However, rather than trying to relate the restoring force to the separation distance through atomic theory, we turn to thermodynamics to see whether there is evidence as the temperature increases for the appearance of further degrees of freedom which might be connected with the population of vibrational states. As shown in Figure 53 there is a rise from  $\frac{3}{2}R$  to  $\frac{7}{2}R$  in  $C_v$  in

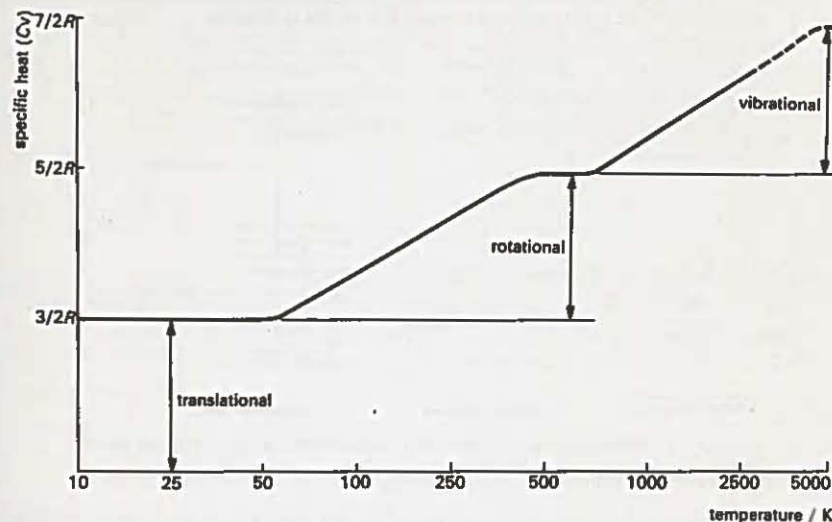


Figure 53 Representation of the variation of specific heat of molecular hydrogen with absolute temperature

the range of temperature around 1500 K. We interpret this rise as being due to the two additional degrees of freedom, one, according to kinetic theory, for the potential energy and one for the kinetic energy, entering as the vibrational states become populated. From the temperature at which the increase takes place we can estimate the vibrational frequency and find

$$\nu_{\text{vib}} = \frac{kT}{h} = 3.12 \times 10^{18} \text{ s}^{-1}.$$

Hence the wave number will be given by

$$k_{\text{vib}} = 1.04 \times 10^2 \text{ mm}^{-1}.$$

We deduce therefore that transitions between vibrational states may give rise to the emission or absorption of quanta in the near infrared. We note that according to equation 9.3 vibrational states are expected to be equally spaced.

Finally, we have the electronic contribution to the molecular energy. As far as the electrons are concerned the situation is not appreciably different from that existing in a simple atom. The electronic states are therefore expected to be such that transitions between them will give rise to quanta of radiation in the visible region of the electromagnetic spectrum.

The description of the diatomic molecule in terms of rotational, vibrational and electronic states fits experimental observations very well. Transitions may be observed directly between rotational levels or directly between vibrational levels; alternatively the existence of these levels may be deduced from the structure that is observed when transitions between electronic states are measured with high resolution. The relationship between the states is illustrated in Figure 54.

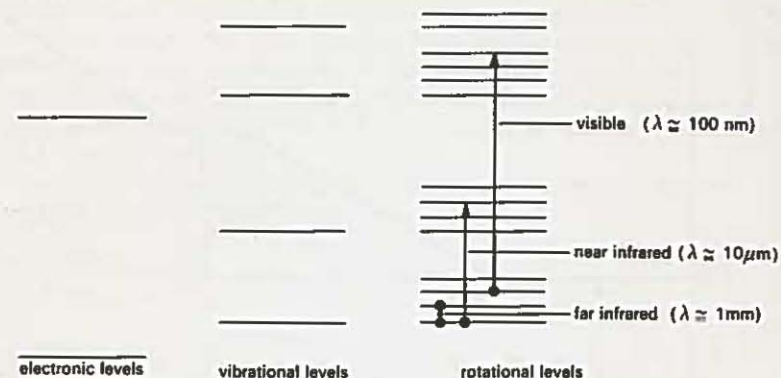


Figure 54 Relationship of electronic, vibrational and rotational levels in diatomic molecule

It should be noted that one reason for the description working so successfully is that the characteristic frequencies associated with the three energy contributions are well separated.

### 9.3 An outline of the collective model of the nucleus

We start by considering a nucleus in which the nucleons are arranged in closed shells. Such a nucleus has spherical symmetry and, should a deformation be impressed on it, forces will act to restore the symmetry. If now a few nucleons be added to form a heavier nucleus, then the shell model is looked on as still providing an adequate description of the nuclear behaviour. Nucleons form pairs which also have spherical symmetry. However, as the process proceeds and the shell is progressively filled, the number of pairs of nucleons increases and the nucleons in the partly filled shell form a 'softer' structure, the restoring forces coming into play when the surface is deformed, being weaker than is the case for a closed shell. Such nuclei are referred to as *transitional nuclei*. As more nucleons are added to the shell, the 'pairing' effect is assumed to become less able to

maintain symmetry and the partly filled shell passes through the state of being an easily deformed sphere and becomes a spheroid or ellipsoid of revolution. Nuclei of this type are called *deformed nuclei*. The subtraction of nucleons from a closed shell can be treated as readily by the shell model as the addition of nucleons, assignments of spins and parities to the 'vacancies' proceeding as for nucleons. Thus as we go on adding nucleons to deformed nuclei we pass into a further range of transitional nuclei before reaching the next closure of the shell. We proceed to develop the consequences of these 'properties' we have conferred on the nucleus.

### 9.4 Rotational states of deformed nuclei

We begin by considering an (even, even) deformed nucleus, i.e. one having an approximately half-filled shell of nucleons. The shape is, as discussed above, no longer that of the spherical closed-shell nucleus but has become that of an ellipsoid of revolution. The extent of the deformation is measured by the ellipticity

$$\epsilon = \frac{c - b}{R_0}$$

where  $c$  is the length of the semi-axis of symmetry and  $b$  the length of the other equal semi-axes.  $R_0$  is  $\frac{1}{2}(c + b)$ . If we take the result derived in section 7.7 for the quadrupole moment of a deformed sphere and use the values of  $\epsilon$  and  $R_0$  defined above, we can write for the intrinsic quadrupole moment of the nucleus we are now discussing

$$Q_0 = Z \frac{2}{3}(c^2 - b^2) = \frac{2}{3} Z \epsilon R_0^2$$

In the present case the nucleus in its ground state has zero angular momentum. Hence, if a direction is specified by an electric field gradient, the spheroid will orient itself randomly, leading, as discussed in section 7.9, to an effective quadrupole moment of zero.

In analogy with a diatomic molecule we now consider the possibility of the nucleus having states in which it rotates as a quantum-mechanical rotator about the axis PQ in Figure 55. This rotation takes place with low enough angular velocity to permit the single-particle orbits, which involve much higher angular velocities, to follow the rotation of the spheroid shape. If, as for the diatomic molecule, we associate a quantum number  $R$  with the rotation, the angular momentum about the axis PQ will be given by  $\sqrt{R(R + 1)} \hbar$  and the energy will be given by

$$\frac{R(R + 1) \hbar^2}{2\mathcal{I}}$$

where  $\mathcal{I}$  is the moment of inertia of the nucleus about the axis PQ.

We now define two sets of orthogonal axes, one set,  $x, y, z$  fixed with respect to the nucleus, the  $z$ -axis being the axis of symmetry, and a set  $x', y', z'$  fixed in the laboratory. If we take  $z'$  as a specified direction then the nucleus will orient

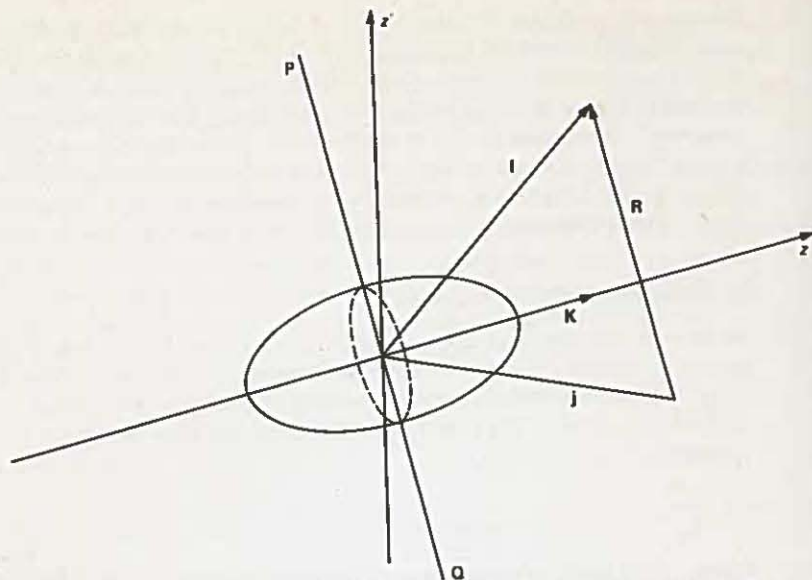


Figure 55 Spheroidal nucleus with intrinsic rotation about  $z$ -axis and capacity for relatively slow rotation about the axis  $PQ$

itself to have a set of magnetic substates, the maximum angular momentum about the  $z'$ -axis being  $R\hbar$ . In this case  $R$  is to be equated to  $I$ , the spin of the excited state of the nucleus. The rotational states are therefore expected in analogy with equation 9.1 to have an energy spacing given by

$$\frac{I(I+1)\hbar^2}{2\mathcal{I}}$$

Since in the case being discussed the spin of the ground state is zero, we note that the rotator is such that a rotation of  $180^\circ$  about the axis  $x$  or the axis  $y$  leaves the system unaltered. In this situation, as for a diatomic molecule with identical nuclei, the states of odd spin are missing and all the states have even parity. The expected states then have spins and parities given by  $0^+, 2^+, 4^+, 6^+, \dots$ , with the energy spacings proportional to  $I(I+1)$ .

It has long been known that, with few exceptions, and these usually associated with closed-shell nuclei, the first excited state of (even, even) nuclei is a  $2^+$  state. The spacing of this state above the ground state diminishes steadily as the shell fills, reaching a minimum with the deformed nuclei. In Table 6 are entered sequences of low-lying states found in four (even, even) deformed nuclei, having spins and parities as predicted above. It is seen that there is a remarkable similarity in energy spacing as between the nuclei, and when the spacing is compared with the theoretical prediction we see that the agreement is good but that there is a growing discrepancy as  $I$  increases. We recall a similar behaviour in the case of

Table 6

Spin and parity	$^{170}_{72}\text{Hf}$	$^{164}_{66}\text{Dy}$	$^{164}_{68}\text{Er}$	$^{166}_{70}\text{Yb}$	$\frac{I(I+1)}{6}$
$16^+$	3.147(31.47)				45.33
$14^+$	2.564(25.64)				35.00
$12^+$	2.013(20.13)			2.172(21.33)	28.17
$10^+$	1.503(15.03)		(1.466)(16.02)	1.604(15.76)	18.33
$8^+$	1.041(10.41)	0.839 (11.43)	1.024(11.19)	1.097(10.77)	12.00
$6^+$	0.641 (6.41)	0.50132 (6.83)	0.614 (6.71)	0.667 (6.55)	7.00
$4^+$	0.321 (3.21)	0.24223 (3.30)	0.299 (3.27)	0.330 (3.24)	3.33
$2^+$	0.100 (1.00)	0.073392(1.00)	0.0915(1.00)	0.1018(1.00)	1.00
$0^+$	0 (0)	0 (0)	0 (0)	0 (0)	0

rotational spectra of molecules, discussed in section 9.2. We assume that the explanation is similar in this case, namely that as the rotational angular velocity increases, the increasing centrifugal force is stretching the nucleus thereby increasing the effective  $\mathcal{I}$  and leading to a reduction in the energy spacing.

We now turn to the case of odd- $A$  nuclei, which, on the single-particle view, have non-zero ground-state spin. Let us assume that the angular-momentum quantum number of the unpaired nucleon is  $j$ . This nucleon will give rise to a component of angular momentum along the  $z$ -axis. This component we denote by  $K\hbar$ . Consider now the rotational states based on this ground state. The angular momentum of rotation will add vectorially to the angular momentum  $\sqrt{j(j+1)}\hbar$  of the unpaired nucleon to give a resultant angular momentum  $I$  with  $|I| = \sqrt{I(I+1)}\hbar$ . The angular momentum of rotation is, from Figure 55, seen to be the component of  $I$  along the axis of rotation and to have a magnitude given by  $\sqrt{I(I+1) - K^2}\hbar$ . It follows that the rotational energy in this case is given by

$$E_{\text{rot}} = \frac{[I(I+1) - K^2]\hbar^2}{2\mathcal{I}}$$

Apart from the term  $-K^2\hbar^2/2\mathcal{I}$ , which will be the same for all the rotational levels in the sequence and therefore will not affect the spacing, we see that this is the same result as was found for (even, even) nuclei. However, the symmetry which suppressed the states with odd spins in that case is not present in the case of odd- $A$  nuclei because  $K$  is no longer zero. Hence we expect the spins of the rotational states to be  $K, K+1, K+2, K+3, \dots$ , all half-integral. The parity of all the states is expected to be the same as the parity of the unpaired particle.

Nuclei having  $K = \frac{1}{2}$  constitute a special case. The angular momentum about the  $z$ -axis is not necessarily unaffected by the rotational motion, and a more complicated treatment beyond the scope of the present discussion is necessary. We simply quote here the result of the theoretical analysis for the case of  $K = \frac{1}{2}$ , namely

$$E_{\text{rot}} = \frac{1}{2}\hbar^2[I(I+1) - K^2 + a(-1)^{I+\frac{1}{2}}(I+\frac{1}{2})], \quad 9.4$$

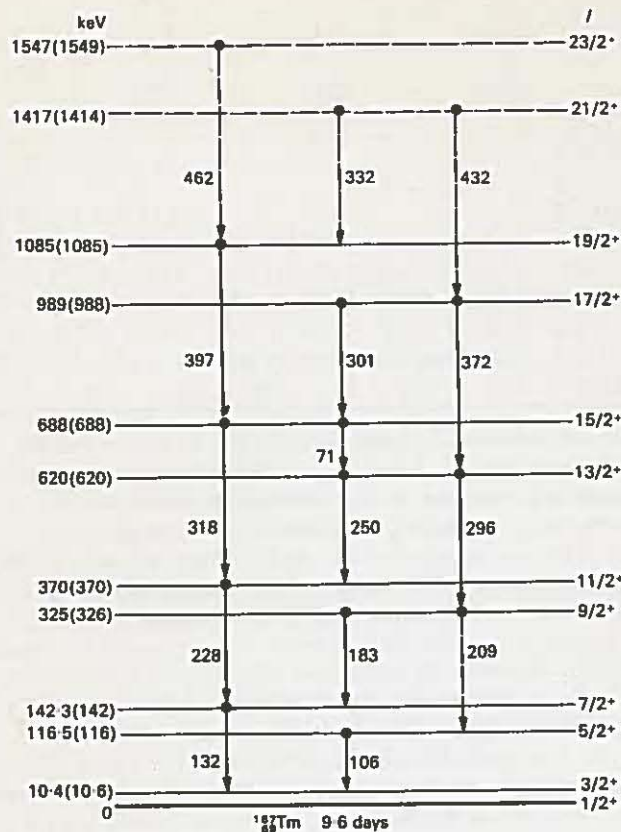


Figure 56 Rotational band of  $^{167}\text{Tm}$ . The energies in parenthesis were calculated from a theoretical formula having four adjustable parameters

where the parameter  $a$ , called the *decoupling parameter*, depends on the details of the intrinsic nuclear structure. In Figure 56 are drawn a sequence of energy levels of  $^{167}\text{Tm}$ . The theoretical estimates based on equation 9.4, with terms added to allow for the stretching in the higher rotational states, show how accurately the model can be made to match the experimental results.

The absolute spacing between states, together with the appropriate formula for  $E_{\text{rot}}$ , can now be used to calculate  $\mathcal{I}$ . The value thus found is considerably less than that which would arise were the nucleons in the nucleus to move around the  $z$ -axis with a common angular velocity. This would amount to a rigid-body rotation of the nucleus and would result in

$$\mathcal{I}_{\text{rig}} = \frac{2}{3}AMR_0^2,$$

where  $M$  is the nucleon mass.

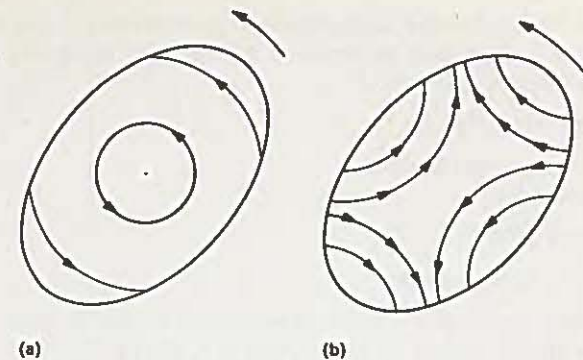


Figure 57 Rotation of spheroid (a) in which all parts move circularly round the axis of rotation as for a rigid body and (b) in which the shape rotates but the component parts oscillate along paths which do not circle the axis of rotation. The latter wavelike rotation corresponds to *irrotational flow*

The measured values however are greater than would arise from a movement of the nucleons depicted in Figure 57, corresponding to irrotational flow in which the surface shape rotates although the individual nucleons do not have a simple circular motion round the axis. In the case of irrotational flow the moment of inertia would be given by

$$\mathcal{I}_{\text{irrot}} = \frac{2}{3}AMR_0^2 \epsilon^2, \quad \text{where } \epsilon = \frac{c-b}{R_0}.$$

The actual behaviour of nucleons, to judge from the measured values of  $\mathcal{I}$ , lies somewhere between the two extremes of rigid-body rotation and irrotational flow.

## 9.5 Vibrational states of nuclei

9.5.1 Corresponding to the linear vibration of the diatomic molecule, we have in the case of the nucleus, the vibration of the three-dimensional sphere (in the case of closed-shell nuclei) or spheroid (in the case of deformed nuclei). In the simplest approach, we assume that the nucleus behaves as if it were an incompressible fluid oscillating under the restoring force of surface tension when deformed in shape. Just as for a vibrating elastic cord fixed at both ends, which is the two-dimensional analogue and more easily visualized, the spherical system is capable of vibrating with one of a series of harmonics or with, in the general case, a mixture of such harmonics. In the case of the sphere, the harmonics are described by functions  $Y(\theta, \phi)$  expressing the displacement of a point  $(R, \theta, \phi)$  on the spherical surface from its initial undisturbed position. The form of the functions  $Y(\theta, \phi)$  has to be found by solving the differential equation corresponding to elastic waves on the spherical surface. This is mathematically similar to the solution of the Schrödinger equation of section 6.3. In place of  $l$  and  $m$  introduced in the separation of the variables in that analysis, we introduce in the present application  $\lambda$  and  $\mu$ . As in the case of a vibrating string, we expect the lowest-order harmonics (i.e. those

described by the lowest  $\lambda$ - and  $\mu$ -values) to have the lowest frequencies and to be associated, in the nuclear context, with the *vibrational states* of lowest energy. We now examine the values of

$$Y_{\lambda\mu}(\theta, \phi) = \Theta_{\lambda\mu}(\theta)\Phi_{\mu}(\phi)$$

for the lowest-order harmonics.

We recall that

$$\Theta_{\lambda\mu}(\theta) = P_{\lambda}^{\mu}(\cos \theta)$$

and take  $\Phi_{\mu}(\phi) = \cos \mu\phi$ ,

rather than the complex function of section 6.4.  $\lambda$  takes the value zero or a positive integer, while  $\mu$ , for a given value of  $\lambda$ , takes positive or negative integral values (or zero) and  $|\mu| \leq \lambda$ . As we are mainly interested in visualizing the modes of vibration, our concern is with the angular dependence of the deformation and we therefore take as unity the constant normalization factor, which strictly speaking ought to occur in the spherical harmonic. The value of the normalization factor controls the relative strength of the particular harmonic being discussed.

(a) For  $\lambda = \mu = 0$ ,  $Y_{00}(\theta, \phi) = 1$ .

This mode constitutes an isotropic expansion or contraction of the spherical shape and, as we are considering the fluid incompressible, the strength of this harmonic must be zero.

(b) For  $\lambda = 1$ ,  $\mu = 0$ ,  $Y_{10}(\theta, \phi) = \cos \theta$ .

The surface in this mode will be described by the equation

$$r = R_0(1 + A \cos \theta).$$

For small values of  $A$  this represents a movement of the whole sphere along the  $z$ -axis without any change in the shape of the surface.

(c) For  $\lambda = 1$ ,  $\mu = \pm 1$ ,  $Y_{1\pm 1}(\theta, \phi) = \sin \theta \cos \phi$ .

For this mode the surface is described by the equation

$$r = R_0(1 + B \sin \theta \cos \phi).$$

Again this represents a bodily movement of the sphere without shape distortion. In this case the centre is displaced in a direction perpendicular to the  $z$ -axis.

(d) For  $\lambda = 2$ ,  $\mu = \pm 1$ ,  $Y_{2\pm 1}(\theta, \phi) = 3 \sin \theta \cos \theta \cos \phi$ .

This vibration, while symmetric with respect to reflection in the origin ( $\phi \rightarrow \phi$ ,  $\theta \rightarrow \pi + \theta$ ), is not symmetrical with respect to reflection in the plane of the  $x$ - and  $y$ -axes ( $\phi \rightarrow \phi$ ,  $\theta \rightarrow \pi - \theta$ ); on the same basis as the rotational states with  $l = 1, 3$ , etc., were discounted above, this mode of vibration is also now discounted.

(e) For  $\lambda = 2$ ,  $\mu = \pm 2$ ,  $Y_{2\pm 2}(\theta, \phi) = 3 \sin^2 \theta \cos 2\phi$ .

This vibration has the necessary symmetry. If we think of the 'poles' of the nucleus lying on the  $z$ -axis with the  $xy$  plane as the equatorial plane, then, as shown in Figure 58, this mode of vibration will involve transport of nuclear mass around the

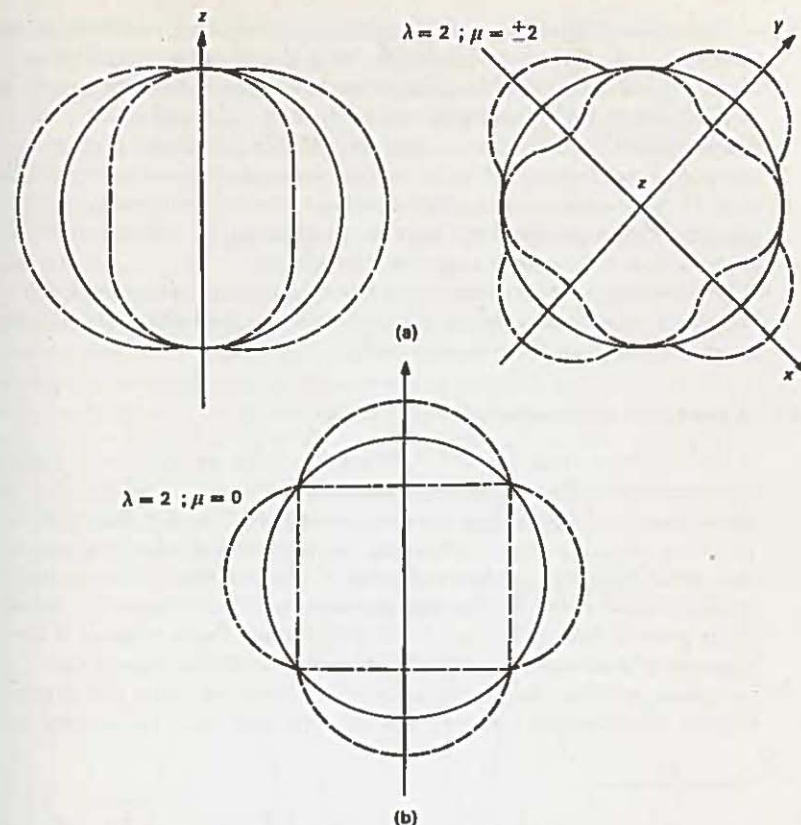


Figure 58 (a)  $\gamma$ -Vibration in which a wave runs equatorially with no variation of polar diameter. (b)  $\beta$ -Vibration in which the polar diameter oscillates with no variation in shape of section at different values of  $\phi$

equator. This will involve angular momentum about the  $z$ -axis amounting in the case of this second-order harmonic to  $2\hbar$  units.

(f) For  $\lambda = 2$ ,  $\mu = 0$ ,  $Y_{20}(\theta, \phi) = \frac{1}{2}(3 \cos^2 \theta - 1)$ .

This vibration also is seen to have the necessary symmetry. From Figure 58 it may be seen that in this mode the transport of mass is towards and away from the poles, i.e. in a plane of constant  $\phi$ . This does not involve the generation of angular momentum about the  $z$ -axis.

The behaviour of the system with respect to angular momentum is therefore seen to be the same as for a particle of spin 2, with  $\lambda$  playing the role of the spin and  $\mu$  playing the role of the magnetic quantum number. The permitted values of the magnetic quantum number in this case being 2 and 0. The energy of vibration is said to be carried by a *phonon* on which we confer these angular momentum properties.

The mode of vibration with  $\lambda = 2, \mu = 0$ , is referred to as a  $\beta$ -vibration; that with  $\lambda = 2, \mu = \pm 2$  is a  $\gamma$ -vibration. The energy levels associated with these vibrations will be spaced as for a simple quantum oscillator, i.e. the spacing will be even. The first level, a one-phonon level, will have spin and parity  $2^+$ . The second level will contain two phonons, each of spin 2. The angular momentum of one phonon will couple with the angular momentum of the other to produce a resultant angular momentum which must have symmetry with respect to the plane  $xy$ . This requirement will limit the resultant angular momentum to the values 0, 2, 4. In all cases the parity will be positive.

The discussion can be continued to take into account more complicated harmonics, for example taking  $\lambda = 3$  will involve octupole vibrations with angular momentum equal to 3 and negative parity.

### 9.5.2 Experimental evidence for vibrational states

In Figure 59 the energy levels of  $^{106}\text{Pd}$  are drawn. We see that there is evidence for the existence of three levels with spins and parities  $0^+, 2^+, 4^+$  at an energy above the ground state of approximately twice that of the first excited state, which has spin and parity  $2^+$ . (We recall that for a rotational band the second state in the sequence has a spin and parity  $4^+$  and an energy 3.33 times that of the first excited state.) We also note that the upper  $2^+$  state decays preferentially to the lower  $2^+$  state rather than to the ground state. This is evidence of the operation of a selection rule typical of harmonic oscillators, namely that transitions between neighbouring states are favoured. We notice that in two respects the theoretical predictions are not accurately borne out, namely that

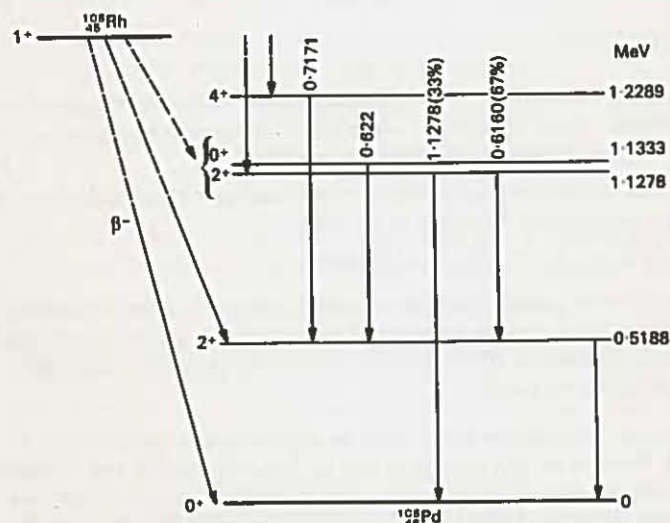


Figure 59 Vibrational states in  $^{106}\text{Pd}$

the two-phonon states are not degenerate and that the energy spacings are not precisely in the ratio 2:1. It has to be remembered that the theory is based on the assumption that the amplitudes of oscillation are within the range of linearity of the restoring forces; this assumption may not be strictly valid.

Many other examples of vibrational states have been found. A study of these reveals that as closed shells are approached the phonon energy increases, indicating that the rigidity of the spherical shape is increasing.

The situation in the case of the nucleus is more complex than it was for a diatomic molecule. The energies of the single-particle states are much closer to the vibrational-state energies than were the electronic-state energies in the case of the molecule. There is thus less validity in the picture of the fast-nucleon orbitals following the relatively slow vibrations of shape of the nucleus. This means that when we come to consider spherical, or nearly spherical, nuclei having odd  $A$ -values there is the complication that the unpaired nucleon has its motion coupled with the vibrations of the core. The results in such cases are then difficult to interpret.

Vibrational states can also arise in deformed nuclei; then the spheroid must be imagined as vibrating as well as rotating. In that case phonons will give rise to vibrational structure which will complicate the rotational bands.

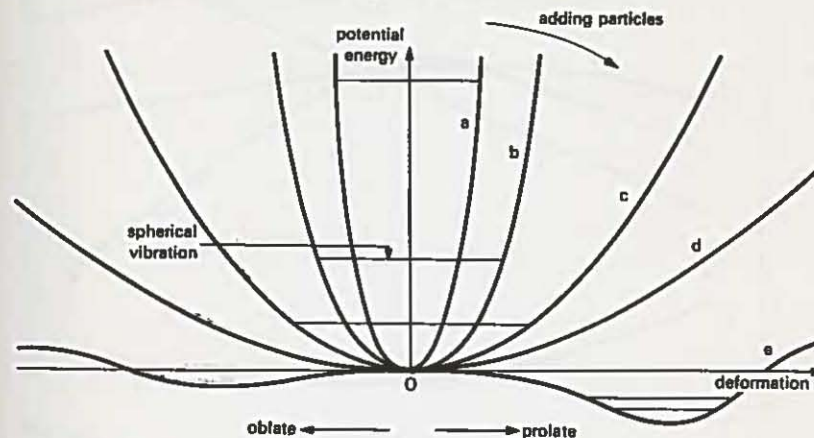


Figure 60 Schematic representation of potential energy as a function of deformation for nuclei ranging from closed shell (a) to permanently deformed (e)

In Figure 60 a schematic representation of the potential energy of the nucleus as a function of deformation summarizes the points that have been made with respect to vibrational levels.

### 9.6 Intrinsic states

In addition to rotational and vibrational states we still have to consider the states of the individual nucleons moving in the average nuclear potential. These correspond to the electronic states in the diatomic molecule. In the case of a

spherical nucleus (i.e. where the shells are filled or almost filled), the individual nucleons experience, as in the simple shell model, a spherically symmetric potential. In the case of the deformed nuclei (i.e. where there is an approximately half-filled shell) the potential will not be spherically symmetric, and the results of section 6.4 will no longer be strictly valid. The analysis of that section has been repeated for an ellipsoidal potential with the results shown in Figure 61. We note that there is further removal of the degeneracies associated with the single-particle states.

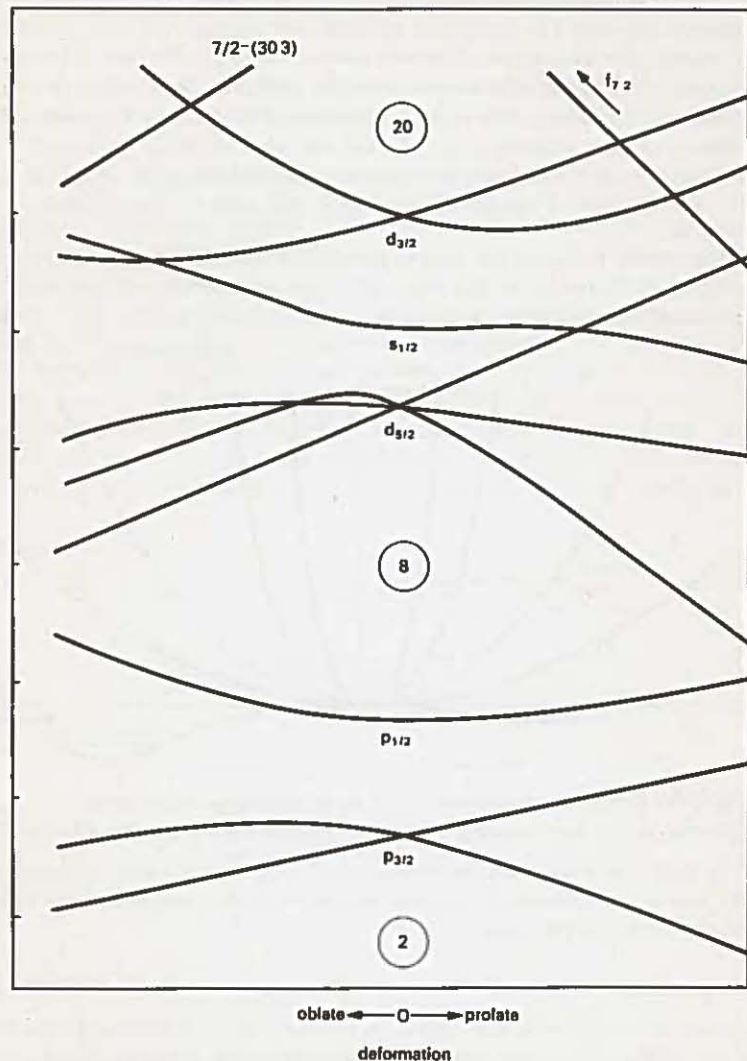


Figure 61 Variation of nuclear energy levels with deformation of nucleus (Nilsson diagram)

## 9.7 Summary

In marshalling the large amount of information now available about the excited states of nuclei we are assisted by the above considerations to the following extent. When we are dealing with a nucleus having closed shells, or almost closed shells, we can seek to interpret the pattern of levels in terms of vibrational states and single-particle states. The latter should be well described by the simple shell model. When we are dealing with nuclei with half-filled, or nearly half-filled, shells, then we have to take into account the deformation of the nucleus. This means that we have the additional possibility of rotational states, and also that the single-particle states will be modified by the fact that the nuclear potential is now axially symmetric but not spherically symmetric.

# Chapter 10

## Excited States of Nuclei

### 10.1 Introduction

In this chapter we discuss the properties of excited states of nuclei. We consider the electromagnetic transitions that occur between states and relate the rates at which these transitions occur to the properties of the states concerned. The methods of measurement and experimental results obtained are briefly reviewed.

### 10.2 Production of excited states

The existence of excited states of nuclei was established, as we saw in section 3.15, by an investigation of the fine structures in  $\alpha$ -particle spectra. The grouping of nucleons which constitutes the daughter nucleus following  $\alpha$ -emission is not always left in its lowest energy state, i.e. in its ground state. Should it be left in a higher energy state, i.e. an *excited state*, then electromagnetic transitions involving the emission of photons take place as the system de-excites.

A similar effect, as noted in section 4.12, is observed in the case of certain  $\beta$ -emitters. In Figure 62 the energy levels in  $^{249}\text{Bk}$  and  $^{93}\text{Zr}$ , constructed from measured  $\alpha$ - and  $\beta$ -spectra, are shown to indicate the number of levels that can be involved and the resulting complexity of the spectrum of  $\gamma$ -rays emitted in association with the  $\alpha$ - and  $\beta$ -particles.

The mass-energy conditions in  $\alpha$ - and  $\beta$ -decay limit the energy range of excitation of the nucleus which is explored by these methods. Even within that limited range, the lower-lying states are favoured in production by the energy dependence of the  $\alpha$ - and  $\beta$ -transition probabilities. Further it is a consequence of the selection rules for  $\alpha$ - and  $\beta$ -decay that only those levels having certain spins and parities will appear in the decay schemes.

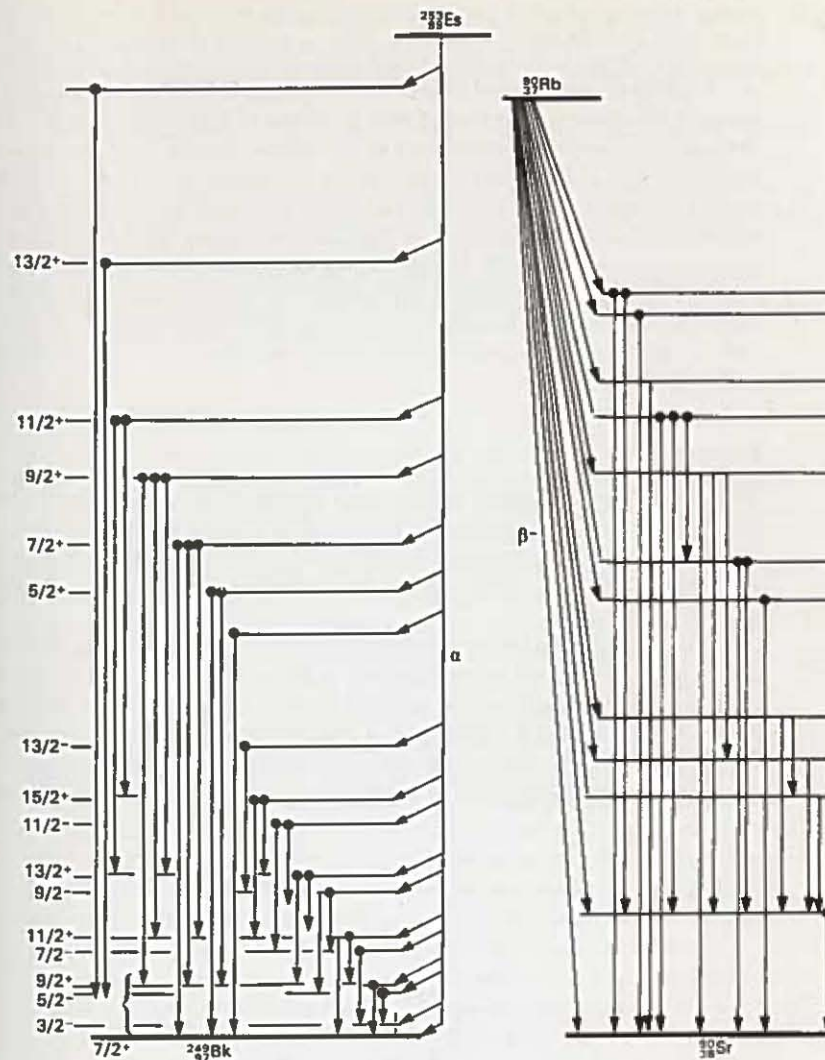


Figure 62 (a) Energy levels of  $^{249}\text{Bk}$  deduced from  $\alpha$ -particle spectrum emitted by  $^{253}\text{Es}$ . (b) Energy levels of  $^{90}\text{Sr}$  deduced from  $\beta^-$  spectrum of  $^{90}\text{Rb}$

### 10.2.1 Photoexcitation

Other methods are now available for the production of nuclear excited states, which enable the energy-level diagrams to be considerably extended. The exposure of a nucleus in its ground state to a beam of high-energy X-rays, produced by stopping the beam from an electron accelerator in a target of a material of high atomic number, can result in the absorption of a photon by the nucleus leading to a transition from the ground state to an excited state. This excited state can lie within an energy range limited only by the energy of the electron producing the X-ray bremsstrahlung spectrum. There are again selection rules involved in the transitions and it is therefore not to be expected that all excited states within the accessible energy range will be populated. We return later to discuss methods involving other nuclear reactions for the production of excited states.

### 10.2.2 Bound states

When the full energy range of excited states is being considered, the states divide into two categories. Those states whose excitation energies are less than the binding energy of the least tightly bound nucleon are termed *bound states*. Those states whose excitation energy exceeds the nucleon binding energy are termed *unbound states*.

Usually a bound state promptly de-excites by  $\gamma$ -ray emission, a process to be considered in some detail below. However, as discussed in section 6.11, there are examples of  $\gamma$ -ray transitions, the so-called isomeric transitions, which proceed at such a slow rate that  $\beta$ -transitions to a neighbouring isobar, where the mass difference permits this process, successfully compete. An interesting example of this is the 2.83 hour state 388 keV above the ground state of  $^{87}\text{Sr}$ , which largely

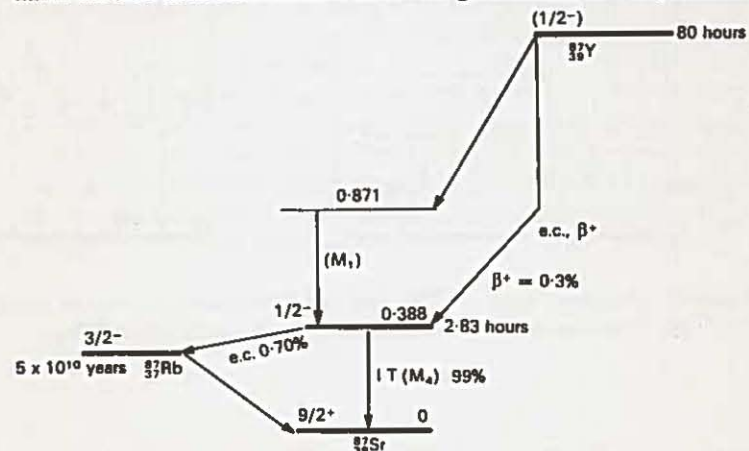


Figure 63 Decay scheme to show the competition between electron capture and  $\gamma$ -ray emission from the isomeric state in  $^{87}\text{Sr}$

de-excites by  $\gamma$ -ray emission to the stable ground state, but in 0.7 per cent of the decays proceeds by electron capture to the ground state of  $^{87}\text{Rb}$ . The decay scheme is shown in Figure 63. This deviation from the normal  $\gamma$ -ray de-excitation is however very rare.

The unbound states of the nucleus have no counterparts in the atomic system. In the case of the atom, as the first ionization energy is passed a continuum of energy states is entered. There is no resonant absorption of photons from the neutral atom ground state into states in this continuum. In the case of the nucleus the behaviour is quite different. Resonant absorption is observed from the ground state to states which lie above the nucleon binding energy. The resulting states may decay by  $\gamma$ -emission but this process usually competes unsuccessfully with nucleon emission, as will be discussed below.

### 10.2.3 Coulomb excitation

Knowledge of excited states has been notably extended in recent years by the exploitation of *Coulomb excitation*. A heavy particle, either a proton or a heavy ion of suitable energy, passing a nucleus in its ground state at a distance greater than the effective range of nuclear forces, gives rise to a transient electric and magnetic field at the nucleus. The resulting perturbation may induce a transition of the nucleus to an excited state. This process, like  $\gamma$ -ray absorption, has the attraction of being entirely electromagnetic in nature and therefore calculable with the aid of the theoretical equipment, in the form of quantum electrodynamics, developed and tested in the field of atomic physics. Coulomb excitation has been particularly successful in demonstrating the existence and determining the properties of the low-lying states associated with rotational bands (see section 9.4). Another technique which has proved extremely valuable in recent years in the study of excited states is electron scattering. A beam of monoenergetic electrons is directed at a target nucleus. The electrons are scattered by purely electromagnetic processes, the scattering events falling into two categories, elastic and inelastic scattering. In an elastic scattering event the nucleus recoils to conserve linear momentum but does not make a transition from its ground state. A comparison of the observed angular distribution of the scattered electrons with that calculated from relativistic quantum electrodynamics, for a given nuclear charge distribution, provides valuable information on the nuclear charge radius. In the event of the nucleus making a transition from its ground state to an excited state the electron scattering is said to be *inelastic*. As in Coulomb excitation, but in this case using the fully relativistic treatment, the transition details are calculable from quantum electrodynamics.

### 10.2.4 The compound nucleus

Coulomb excitation and electron inelastic scattering are two specialized forms of nuclear reactions by means of which both bound and unbound excited states may be populated. In the more general form of nuclear reaction, where the bombarding

